Probabilistic Assessment of the Failure of Laminated Timber Bridges

LESLIE G. JAEGER and BAIDAR BAKHT

ABSTRACT

For a given loading, the ratio of the expected failure load of a laminated timber bridge and the analytical failure load obtained by assuming the modulus of rupture (MOR) and modulus of elasticity (E_L) to obtain their respective mean values, is called the reduction factor. The value of this factor is always less than 1.0, and depends on the transverse deflection profile of the bridge. A procedure is presented in this paper by which a realistic assessment of the reduction factor can be obtained by using test data for the MOR and E_L for any species of wood.

There are two properties of timber beams that have a marked effect on the distribution of live loads in laminated timber bridges and on the ultimate load-carrying capacity of such bridges; these are the modulus of elasticity (E_L) and the modulus of rupture (MOR).

The E_L and MOR vary widely from one timber beam to another. Figure 1 shows test values of E_L and MOR on 70 Red Pine specimens. These values were originally given in an unpublished report of the Ontario Ministry of Transportation and Communications, and were used recently in Bakht and Jaeger (1). As will be seen from Figure 1, E_L and MOR are strongly correlated, but not perfectly so. If they were perfectly correlated, all points in Figure 1 would appear on a single line. The variability in E_L and MOR, and, more particularly, the variability in E_L/MOR, has the effect of significantly reducing the ultimate load-carrying capacity of the bridge, as compared to what it would be if all beams had the same E_L and MOR, equal to their mean values for the species concerned. This significant reduction can be related to the amount of scatter that is shown in Figure 1. The reduction factor is also dependent on the deflection profile of a cross-section of the bridge. In this paper, only the estimation of the expected load capacity is dealt with; estimation of the variance of this capacity is dealt with elsewhere.

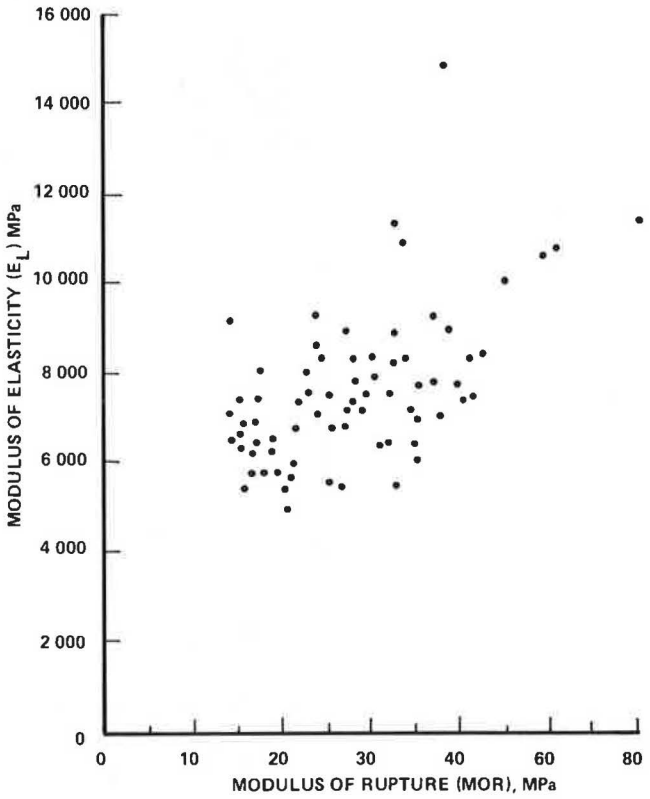

FIGURE 1 Test data on 70 Red Pine specimens.

DERIVATION OF THE METHOD OF ANALYSIS

As a first step, the values of E_L and MOR given in Figure 1 are replotted on axes of $E_L/(E_L)_{mean}$ and $MOR/(MOR)_{mean}$ as shown in Figure 2. Then, for a given species of timber, the scatter of points can be approximated as lying within an area bounded by $r = r_1$ and $r = r_2$ and by $\theta = \alpha$ and $\theta = (90°-\alpha)$, where r is a radial distance from the origin and θ is an angle measured clockwise from the $E_L/(E_L)_{mean}$ axis, as shown in Figure 2. For Red Pine, the angle α is about 30°. It will be shown later that the limiting values r_1 and r_2 do not need to be estimated.

The behavior depicted in Figure 2 may be contrasted with that of Figure 3, which shows what happens if the values of E_L and MOR are assumed to be perfectly correlated (i.e., if E_L/MOR is assumed to be constant). It will be seen that the imperfect nature of the correlation that occurs with Red Pine results in a "fan" of points rather than a single line.

The scatter of points over the area of Figure 2 is represented by a probability density function $p(r,\theta)$, which satisfies the relationship

$$\int_{\alpha}^{(\pi/2)-\alpha} \int_{r_1}^{r_2} p(r, \theta)\, r\,dr\,d\theta = 1 \qquad (1)$$

For simplicity, two further assumptions are made about the nature of the points in Figure 2. These

L.G. Jaeger, Technical University of Nova Scotia, Halifax, Nova Scotia, Canada. B. Bakht, Ministry of Transportation and Communications, Downsview, Ontario, Canada.

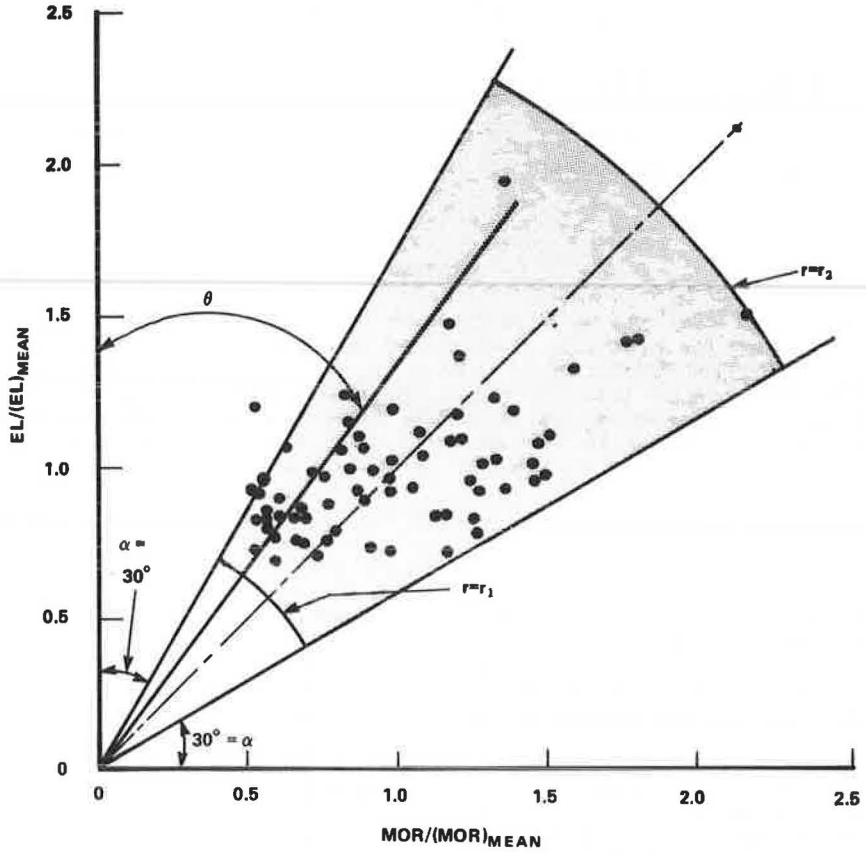

FIGURE 2 Data on Red Pine wood.

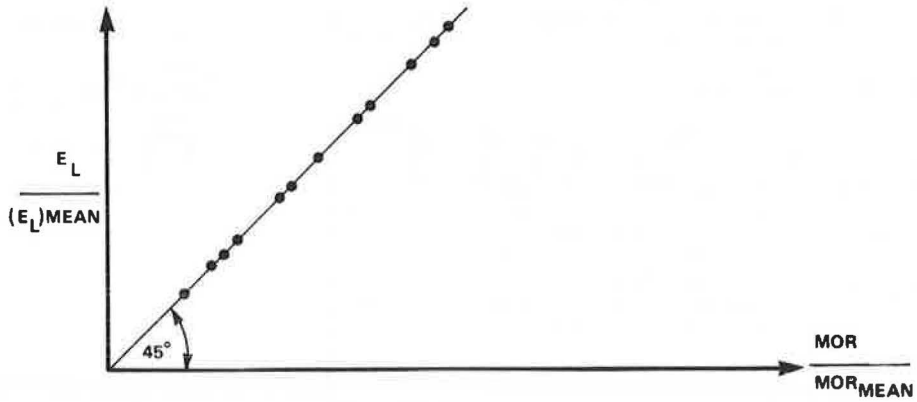

FIGURE 3 Perfect correlation of E_L and MOR.

are that the probability distribution can be split up into "variation with θ" and "variation with r" and that the "variation with θ" is symmetrical about the line θ = 45°. Both of these assumptions are reasonable in light of the observed test values for different species of timber.

It is fortunate for the purposes of estimation of failure load that the analysis is not sensitive to the precise form of the probability function p(r,θ) that is chosen. (This point will be returned to later.) The general nature of the probability distribution p(r,θ) is shown in Figure 4. Then,

$$p(r,\theta) = f(r)\phi(\theta) \quad (2)$$

where

$$\int_{r_1}^{r_2} f(r)\,dr = 1 \quad (3)$$

and

$$\int_{\alpha}^{(\pi/2)-\alpha} \phi(\theta)\,d\theta = 1 \quad (4)$$

Figure 5 shows the general nature of the probability functions φθ. This function must be zero outside the range of values α and (90°−α) and be symmetrical about θ = 45°. A suitable form for the purpose of analysis is

$$\phi(\theta) = c(\sin 2\theta - \sin 2\alpha) \quad (5)$$

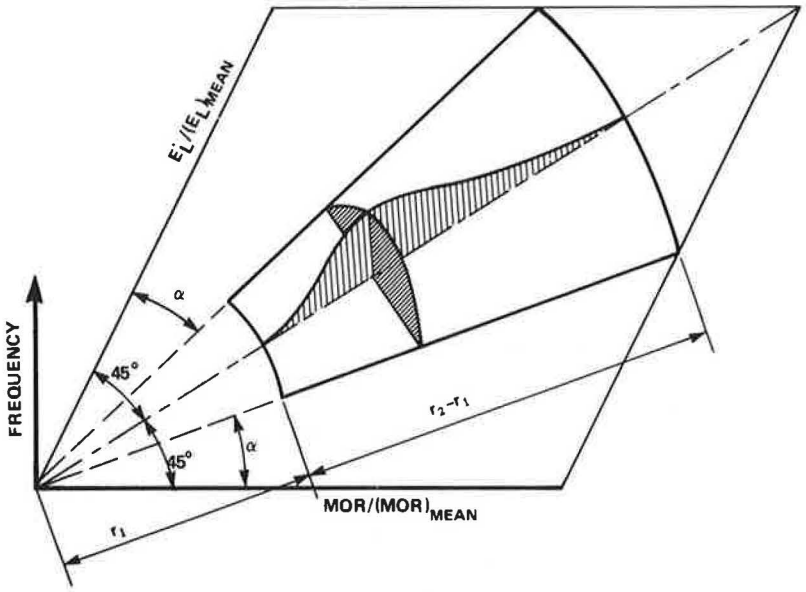

FIGURE 4 The probability function $p(r,\theta)$.

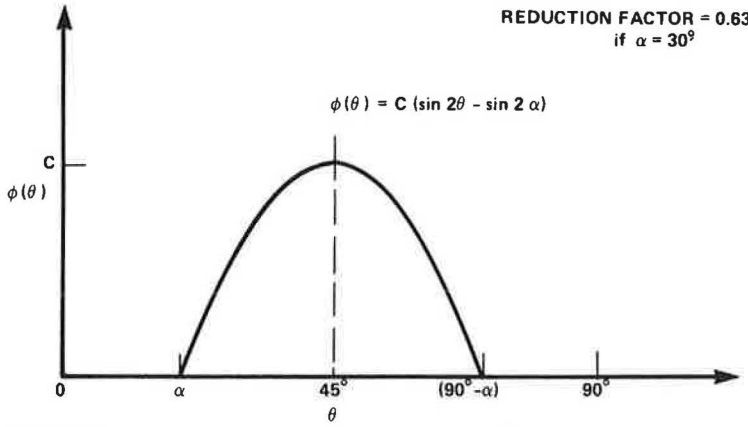

FIGURE 5 Plot of $\phi(\theta)$ against θ.

for

$$\alpha \leq \theta \leq 90° - \alpha$$

The constant c in Equation 5 is readily found by using Equation 4. In the case of Red Pine, taking $\alpha = 30°$ the following is obtained:

$$\phi(\theta) = 21.488[\sin 2\theta - (3^{1/2}/2)] \quad (5a)$$

Having derived the necessary properties of the scatter of pairs of values of E_L and MOR, an investigation of ultimate failure loads for various patterns of transverse deflection can now be undertaken. For each pattern of deflection, the actual expected value of ultimate failure load is related to the deterministic failure load that is obtained by taking all beams to have the same E_L and MOR, being the mean value for the timber species concerned. As a preliminary, it may be noted that the ultimate failure load, M_{ult}, of a beam is directly proportional to its MOR. Hence, in Figure 2, the horizontal axis can be $M_{ult}/(M_{ult})_{mean}$ as well as MOR/$(MOR)_{mean}$.

THE CASE OF UNIFORM DEFLECTION

The first pattern of transverse deflection that is examined is that of uniform deflection, shown in Figure 6. If all beams are taken to be identical, then as the uniform deflection increases, the bending moments accepted by the beams increase until all beams simultaneously reach $(M_{ult})_{mean}$. Hence, in the deterministic approach, the total ultimate bending moment capacity of the bridge is simply

$$M_T = N(M_{ult})_{mean} \quad (6)$$

When the scatter of values of E_L and MOR is taken into account, a different behavior emerges. The beams do not fail simultaneously. Because all beams deflect equally, the moment accepted by a beam is proportional to its own E_L, and its ability to withstand moment is proportional to its own value of MOR (or, alternatively, its own value of M_{ult}). The first beams to fail, therefore, are those with the lowest value of MOR/E_L. Figure 7 is a repetition of Figure 2 with the addition of a failure boundary at $\theta = \beta$. As the uniform deflection shown in Figure 6 increases, a

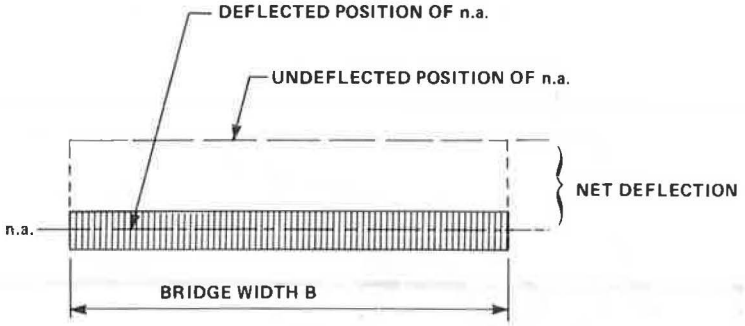

FIGURE 6 Uniform deflection across a bridge cross-section.

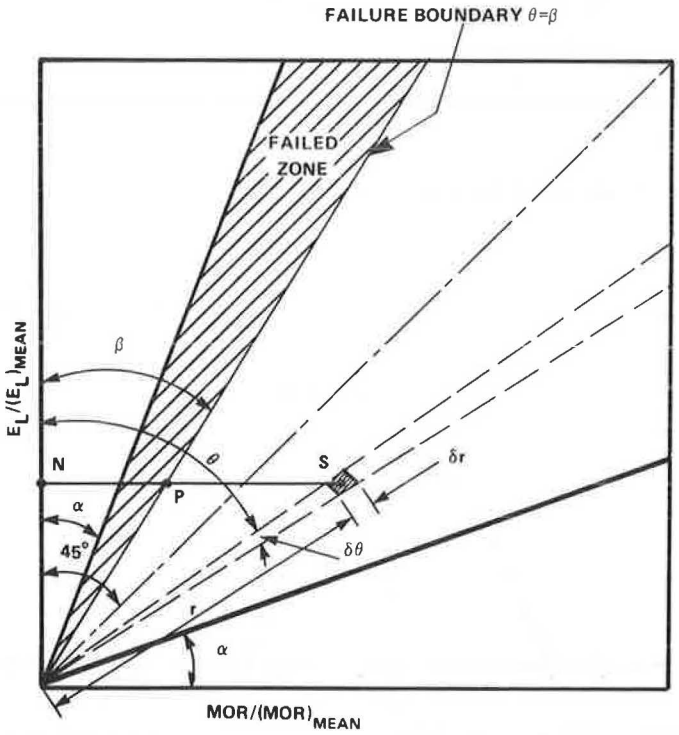

FIGURE 7 Failed zone.

radial line (starting at the vertical axis) rotates clockwise in Figure 7. For a certain deflection, all of those beams to the left of the boundary in Figure 7 have already failed, although those to the right have not. Similarly, in Csagoly and Taylor (2), it is assumed that when a beam's ultimate moment capacity has been reached, the beam fails and its moment carrying capacity falls to zero.

The total bending moment being accepted by those beams that have not yet failed is readily found. The small element $r\delta r\delta\theta$ shown at the point S in Figure 7 is considered. The number of beams expected in this area is $NP(r,\theta)r\delta r\delta\theta$. These beams are not yet at their failure moments, however; they are, in fact, taking a fraction (NP/NS) of their failure moments, with the notation of Figure 7. This follows because all beams having the same value of E_L take the same moments as one another until failure. Using the notation shown in Figure 7,

$$NP = r\cos\theta\tan\beta \tag{7}$$

The bending moment accepted by the beams in the shaded area $r\delta r\delta\theta$ is

$$\delta M = \{Np(r,\theta)r\delta r\delta\theta\}r\cos\theta\tan\beta(M_{ult})_{mean} \tag{8}$$

Using Equations 2-4, and 6, and integrating Equation 8

$$M = M_T\tan\beta \int_{r_1}^{r_2} f(r)r^2dr \int_{\beta}^{(\pi/2)-\alpha} \cos\theta\phi(\theta)d\theta \tag{9a}$$

which is conveniently written as

$$M = k(\beta)M_T \tag{9b}$$

where

$$k(\beta) = \tan\beta \int_{r_1}^{r_2} f(r)r^2dr \int_{\beta}^{(\pi/2)-\alpha} \cos\theta\phi(\theta)d\theta \tag{9c}$$

The calculation of $k(\beta)$ using Equation 9c is straightforward and is greatly simplified by the fact that the function $f(r)$ does not need to be found explicitly. In fact, the value $\int_{r_1}^{r_2} f(r)r^2dr$ can be

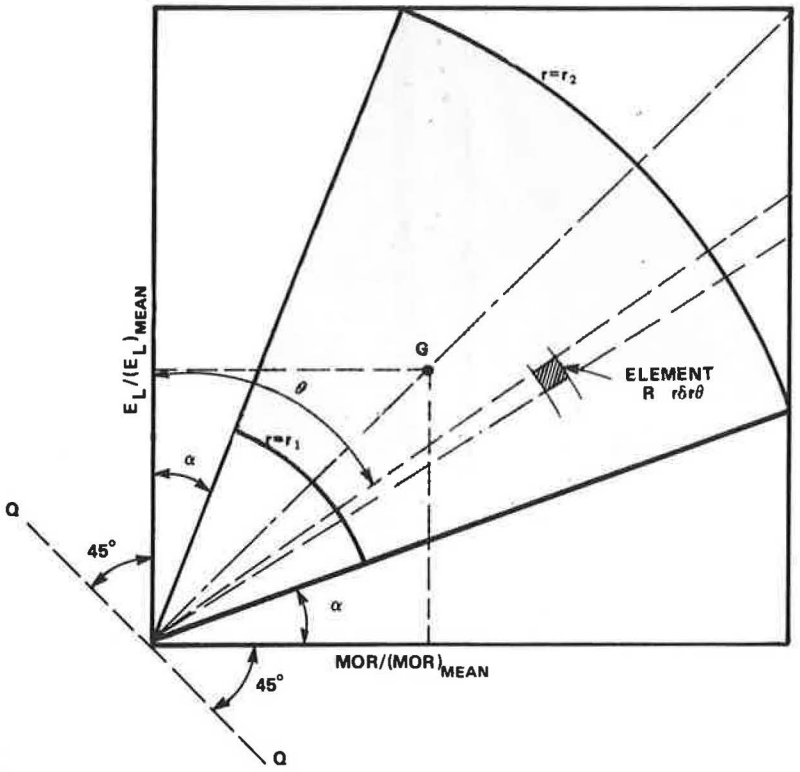

FIGURE 8 Evaluation of $\int_{r_1}^{r_2} f(r)r^2dr$.

determined from knowing the position of the center of gravity of the probability distribution. (Details of the evaluation of Equation 9c are given in Jaeger and Bakht (3) and an evaluation is shown in Figure 8.

It is also shown in Jaeger and Bakht (3) that the expression for k(β) can be simplified, on eliminating the integral with respect to r, to

$$k(\beta) = \{2 \tan \beta \int_{\beta}^{[(\pi/2)-\alpha]} \cos \theta \, \phi(\theta) \, d\theta \div \int_{\alpha}^{[(\pi/2)-\alpha]} (\sin \theta + \cos \theta) \, \phi(\theta) \, d\theta\} \quad (9d)$$

where k(β is readily evaluated from) Equation 9d for any assumed $\phi(\theta)$.

Although the details of the mathematics may not be of much interest to engineers, the underlying physics of how the collapse builds up certainly are. Referring again to Figures 6 and 7, for small values of deflection, the boundary $\theta = \beta$ does not go through the area defined by the scatter of points. As deflection continues to increase, and the radial line continues its motion, a stage is reached at which the radial line reaches the angular position α of Figure 7. From that point on, the most vulnerable beams (i.e., those with the smallest values of MOR/E_L) begin to fail. For a time, increasing values of deflection, and the corresponding increases in the angle β, are accompanied by further increases in the load-carrying capacity, but the rate of increase decreases steadily. Eventually, a value of β is reached for which k(β) is a maximum, after which it reduces. The maximum value of k(β) gives the failure state of the bridge, in accordance with Equation 6.

The equation for k(β) is given as

$$k(\beta) = 30.588 \tan\beta (2/3 \cos^3\beta + 3^{1/2}/2 \sin\beta - 5/6) \quad (10)$$

for values of β greater than 30° for Red Pine (3).

Figure 9 is a graph of ultimate load factor k(β) plotted against the angle β. The maximum is reached when β is 0.62 radians (i.e., 35.52°), at which point k(β) has the value 0.639. Hence, for Red Pine in uniform deflection,

$$M = 0.639 \, M_T = N \{0.639 (M_{ult})_{mean}\} \quad (11)$$

From Equation 11, the ultimate failure load of the bridge is reduced (because of the scatter of values) to 0.639 of what it would have been if all beams had had the same M_{ult}--that is, if all had had $(M_{ult})_{mean}$, and the same value of E_L--that is, $(E_L)_{mean}$. It should be emphasized that the reduction in the ultimate failure load as estimated by Equation 11 is not brought about by having beams that are, on the average, weaker than usual. The beams are taken to have an average strength that is entirely normal, and it is the scatter of (MOR/E_L) above and below the mean that gives rise to the progressive failure of the bridge and the reduction in its ultimate load-carrying capacity as compared with the "no scatter" situation.

The reduction factor of 0.639 that appears in Equation 11 is derived from the probability distribution of the quantity (MOR/E_L), and the ultimate failure moment M given by Equation 11 is, in fact, the mean value (i.e., the expectation) of a random variable. The derivation of a failure load for design purposes also requires the determination of the standard deviation of this random variable. That determination is given in Jaeger and Bakht (3). It

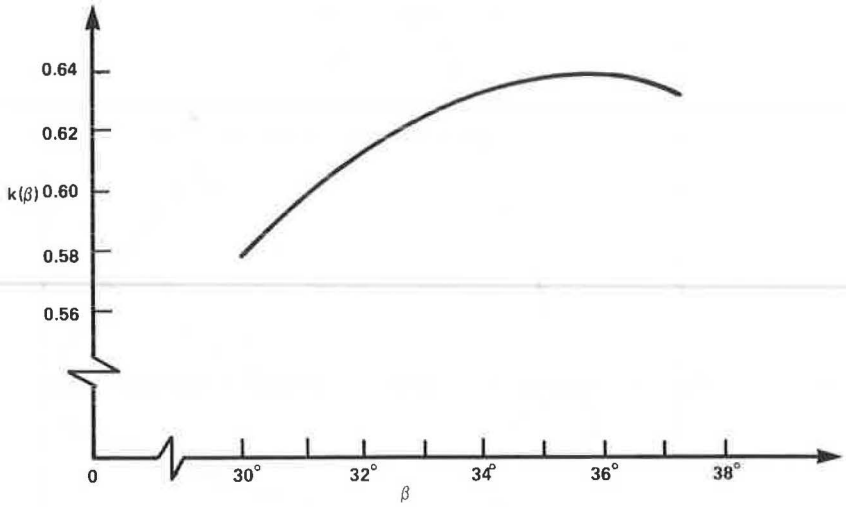

FIGURE 9 Plot of k (β) against β.

is sufficient to note here that for laminated timber bridges, the Number (N) of beams is large and, hence, the variability of the ultimate failure load about the mean value given by Equation 11 is small. It is instructive to repeat the preceding analysis for other assumed probability distributions. Fortunately, the reduction factor is found to be not sensitive to such changes; for example, if the function $\phi(\theta)$ is assumed to be constant for values of θ between α and $(90°-\alpha)$ as shown in Figure 10, even this quite marked change only has the effect of lowering the reduction factor to about 0.577 when $\alpha = 30°$.

Figures 5, 10, and 11 clearly bring out one important point. This is that the shift from the perfect correlation case of Figure 11 to either Figures 5 or 10 gives a change in reduction factor from 1.00 to 0.639 or 0.577, which is much larger than the difference between the latter two. This confirms that a

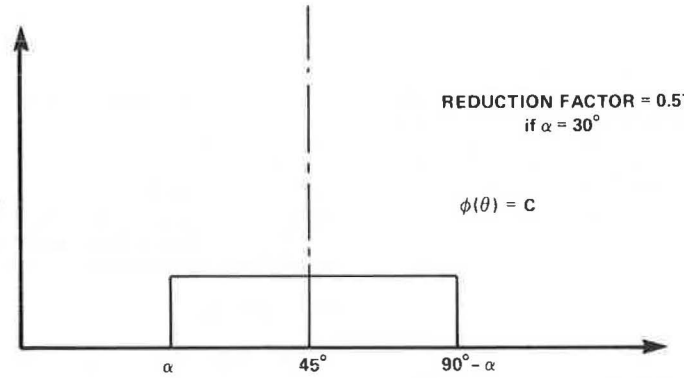

FIGURE 10 An extreme assumption for $\phi(\theta)$.

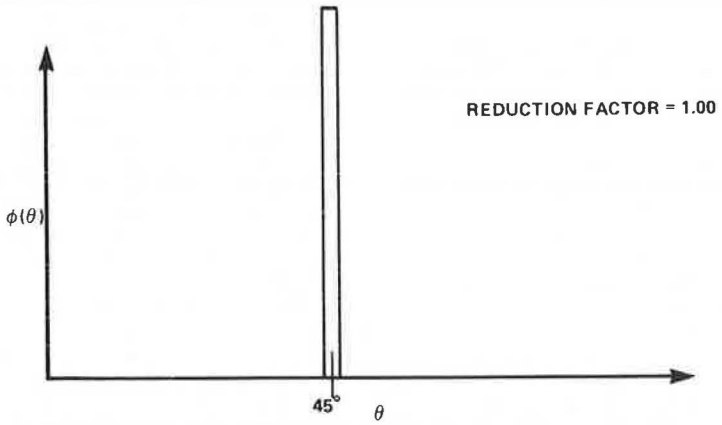

FIGURE 11 The plot of $\phi(\theta)$ for perfect correlation of E_L and MOR showing an indefinitely high spike of vanishing width—Dirac Delta Function.

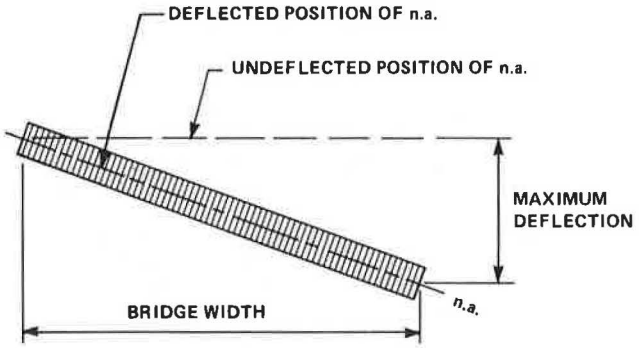

FIGURE 12 Linear deflection across a bridge cross section.

fairly good estimate of the reduction factor can be obtained by taking a reasonable representation of the scatter with respect to θ.

THE CASE OF LINEARLY VARYING DEFLECTION

The adoption of a completely uniform deflection pattern across a transverse cross-section is, of course, a highly idealized case, which can be regarded as one extreme. For purposes of comparison, the second deflection pattern considered is that of Figure 12, in which the deflection is assumed to vary in a straight-line manner from zero at one side of the bridge to a maximum value at the other. If all beams are taken to be identical with $(E_L)_{mean}$ and ultimate moment $(M_{ult})_{mean}$, then failure is reached when the deflection of the right-hand end reaches the value that gives $(M_{ult})_{mean}$ at that end.

Again, in making the assumption that the moment of resistance of a failed beam falls immediately to zero, it is readily seen that attainment of $(M_{ult})_{mean}$ at the right-hand end leads at once to the collapse of the bridge and that

$$M_T = 0.5N\ (M_{ult})_{mean} \tag{12}$$

In Equation 12, the factor 0.5 arises from the linear variation of deflection across the cross-section. The estimation of total failure moment for this deflection pattern [taking into account the scatter in values of (MOR/E_L)] follows the same general line as that for the uniform deflection cases, except that now each element of the cross-section has its own deflection and, hence, its own radial line on the plot of Figures 2 and 3. Figure 13 shows the situation in which the deflection of the right-hand end gives the radial line $\theta = \beta$. Then, a width $B(\tan\alpha/\tan\beta)$ of the cross-section is known to be still unfailed, although the right-hand portion of the cross-section is composed of elements that have increasing probabilities of failure as one moves from left to right. [Details of the estimation of the ultimate failure moment are given in Jaeger and Bakht (3).] In the case of Red Pine, the result is

$$M = 0.415\ N\ (M_{ult})_{mean} \tag{13}$$

In this case, it is seen from Equations 12 and 13 that the reduction factor in ultimate load-carrying capacity is 0.830, as compared to 0.639 in the case of a uniform deflection. This relatively better performance is entirely to be expected because with the pattern of deflection now assumed, a fairly large fraction of the cross-section is known to be not involved in the initiation of failure, so that the

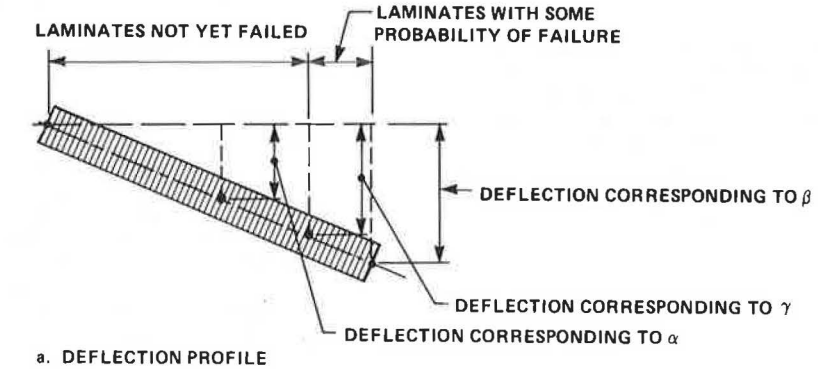

a. DEFLECTION PROFILE

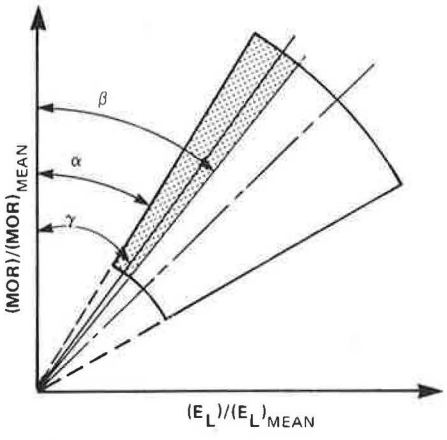

b.

FIGURE 13 Identification of failure zone.

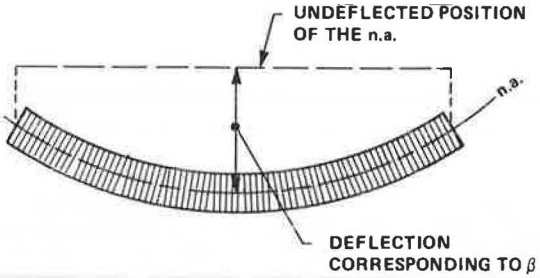

FIGURE 14 A nonuniform deflection pile.

influence of the scatter of values of (MOR/E_L) is much reduced.

The procedure for estimating ultimate moment capacity for any general deflection pattern, such as that shown in Figure 14, follows the same steps. The maximum deflection of the cross-section corresponds to a radial line $\theta = \beta$ in the plot of Figure 7. Any other point on the cross-section has a radial line $\theta = \lambda$ where $(\tan\lambda/\tan\beta)$ is the ratio of deflections for the two points concerned. Estimation of the ultimate moment capacity then follows using the method given in Jaeger and Bakht (3). In practice, the reduction factor for a uniform deflection, which is 0.639 in the case of Red Pine, is found to be the lowest reduction factor that occurs.

CONCLUSIONS

The failure loads of laminated timber bridges cannot be safely estimated by treating all of the beams as having the same (average) E_L and MOR. For Red Pine, a safe estimate of failure load is about 60 percent of the failure load obtained in that way. The estimate of failure load is not sensitive to the probability distribution that is assumed; provided that this distribution is fairly near the truth, the reduction factor that is due to the progressive nature of collapse can be predicted with reasonable accuracy. It is noted that this paper deals with estimation of the expectations of failure load (i.e., with estimation of the mean value of a random variable). The estimation of the standard derivation of this random variable is outlined elsewhere (3).

NOTATION

Following is a list of definitions for the variables used in this paper.

E_L = modulus of elasticity of a timber beam in the longitudinal direction;

$(E_L)_{mean}$ = mean value of E_L for the species of timber concerned;

MOR = modulus of rupture of a timber beam;

$(MOR)_{mean}$ = mean value of MOR for the species of timber concerned;

$E_L/(E_L)_{mean}$ = coordinate axes for representation of probability distribution of a given species of timber;

$MOR/(MOR)_{mean}$ = coordinate axes for representation of probability distribution of a given species of timber;

(r,θ) = polar coordinates in the plane of $E_L/(E_L)_{mean}$ and $MOR/(MOR)_{mean}$, with θ being $E_L/(E_L)_{mean}$;

$p(r,\theta)$ = a probability distribution;

α = minimum value of θ for which the probability function $p(r,\theta)$ has non-zero values;

$f(r)$, $\phi(\theta)$ = variations of $p(r,\theta)$ in the r and θ directions, respectively;

β = the value of θ corresponding to the maximum deflection in the cross-section of a bridge; that is the maximum value of λ; and

λ = the value of θ corresponding to the deflection of a representative point on the cross-section of a bridge.

ACKNOWLEDGMENTS

The authors wish to acknowledge the Natural Sciences and Engineering Research Council of Canada and the Ontario Ministry of Transportation and Communications for their support in this research.

REFERENCES

1. B. Bakht and L.G. Jaeger. Computer Simulation of Failure in Timber Bridges. Proc., 2nd International Conference on Computer Methods in Civil Engineering, Hangchow, China, June 1985.
2. P.F. Csagoly and R.J. Taylor. A Structural Wood System for Highway Bridges. International Association for Bridge and Structural Engineering, Periodica, No. 4, 1980, pp. 157-183.
3. L.G. Jaeger and B. Bakht. Ultimate Failure Loads of Timber Bridges. Structural Research Report 85-04. Ministry of Transportation and Communications, Downsview, Ontario, Canada, Sept. 1985.